PAPER 68 – DEVELOPMENT OF ACTIVATED CARBONS FROM *PENTACLETHRA MACROPHYLLA* PODS AS HIGH-PERFORMANCE ADSORBENT FOR TREATMENT OF AZO DYE WASTEWATER

Gabriel O. Ogbeh[1*], Ayodele O. Ogunlela[2], and Raphael T. Iwar[1]

[1]Department of Agricultural and Environmental Engineering, Joseph Sarwuan Tarka University, P.M.B. 2373 Makurdi, Nigeria
[2]Department of Agricultural and Biosystems Engineering, University of Ilorin, Nigeria
[*]Email: gabriel.ogbeh@uam.edu.ng

ABSTRACT

This present study reports the preparation of activated carbons via facile pyrolysis using African oil bean (*Pentaclethra macrophylla*) pods as a potential carbon precursor. The experimental process parameters were optimized through a chemometric tool to produce activated carbons of high carbon yield and iodine numbers with H_3PO_4 and KOH as activating agents. The results indicated that the activated carbon obtained using KOH (KOH-$PMAC_{op}$) has a moderately higher surface area of 911.70 m^2/g than 527.59 m^2/g obtained using H_3PO_4 (H_3PO_4-$PMAC_{op}$) on almost the same set of optimum production parameters. It also exhibited the highest adsorption capacity of 148 mg/g for Congo red. Both activated carbons demonstrated evidence of extensive graphitic features from the analyses of the Raman spectroscopy and X-ray diffraction investigations conducted on them. The Fourier transform infrared (FT-IR) spectra of the KOH-$PMAC_{op}$ suggested a higher proportion of aromaticity than that of H_3PO_4-$PMAC_{op}$, which implies that it is likely to promote adsorption mechanisms like electrostatic and π-π interactions far better than that of H_3PO_4-$PMAC_{op}$. Both carbons, however, suggested their ability to support any rate-controlling chemisorption mechanism, as indicated by the Pseudo-second-order kinetic model obtained from the experimental data. Using African oil bean pods as a precursor for activated carbon offers another chance to develop sustainable and high-efficient adsorbents for wastewater treatment.

KEYWORDS: Activated carbons, Azo dye wastewater, Chemical activation, Chemometric tool, *Pentaclethra macrophylla* pods

1 INTRODUCTION

Wastewater from dyeing industrial processes constitutes one of the global environmental risk concerns. The discharge of dyeing wastewater into surface water resources impairs their quality parameters which are mostly occasioned by incomplete degradation of dye, as the inherent colour impedes light penetration into the water bodies (Karuppasamy *et al*., 2021; Yeow *et al*., 2021). The discharge of dyeing wastewater on soils also causes soil infertility, as the dye tends to stabilize and retain soils (Chandanshive *et al*., 2018; Hassan *et al*., 2022). Delays of seed germination and even plant growth inhibition on soils irrigated with dyeing wastewater have been reported (Chandanshive *et al.*, 2018; Khan & Malik, 2018). Many dyes are also known to be harmful to animal and human health, especially upon prolonged exposure, as they cause allergies, respiratory disorders, irritation, and even mutations or cancer risks in some cases (Chung, 2016; Kadhom *et al*., 2020). It is therefore imperative to facilitate the removal of dyes from wastewater at the source of generation before its eventual discharge into large bodies of water or on land. Although advanced treatment systems such as photocatalysis, the Fenton process, electrooxidation, and biological treatment have been successfully used to treat dye wastewaters, these treatment systems are often expensive to operate and maintain (Asaithambi *et al*., 2022; Bilińska & Gmurek, 2021; Solayman *et al*., 2023; Yeow *et al*., 2021). Due to its comparatively high efficiency, cost-effectiveness, and environmental friendliness, an activated carbon-based adsorption system has recently taken the lead as the preferred method for the treatment of dyeing wastewater.

Commercial activated carbons (ACs) are still expensive to buy, thus research on finding low-cost precursors for their synthesis has become more important (Ajaelu *et al*., 2022; Nindjio *et al*., 2022). The physical activation method, involves carbonization and activation in two steps (Ogungbenro *et al*., 2017; Yang *et al*., 2010), the chemical activation method, which transforms cellulose structures into carbonaceous material through simultaneous dehydration and carbonization (Jaria et al., 2019; Yorgun & Yildiz, 2015), the combined physical and chemical activation method, or the microwave-assisted activation method (Ao *et al*., 2018; Lam *et al*., 2017; Liew *et al*., 2018), are the different ways that activated carbons are produced. The chemical activation method offers the advantage of allowing the production of activated carbons of higher qualities at lower cost due to its lower power required to generate the needed activating temperatures, typically ranging from 400 to 700°C (Loredo-Cancino *et al*., 2013). The chemical activation method is, however, beset with the challenge of selecting the most appropriate optimal production conditions required to produce activated carbons of desired qualities. Because of their renewability and low cost, agroforestry wastes are appealing precursors for the sustainable

production of ACs. The creation of ACs with desirable qualities is influenced by a few factors, including the properties of the precursors, the manufacturing procedure, and the activation agents (Kwiatkowski & Broniek, 2017; Li *et al*., 2017). Depending on the content, stability, presence of heteroatoms, and functional groups of the plant waste, different ACs will be produced (Ekpete *et al*., 2017; Hidayu & Muda, 2016; Shamsuddin *et al*., 2016). Numerous widely available agroforestry residues have been explored for their potentials as ACs precursors. The pod of the African oil bean (*Pentaclethra macrophylla*) tree is one of such biomaterials. The African oil bean tree belongs to the Leguminoseae family and the Mimosoideae subfamily and grows approximately 6 meters in girth and 21 meters in height (Okpala, 2015). The most widely used part of the African oil bean tree is the seeds, which are usually enclosed in some flat pods that tend to burst once matured thereby dispersing the seeds. The pods are often considered waste and remain underused. The pods measure about 35 to 45 centimetres long by 5 to 10 centimetres broad, black in colour, quite hard, and woody in appearance.

There have been a few studies looking into the effects of preparation variables like temperature and impregnation ratio on activated carbons (ACs) from *Pentaclythra macrophylla* pods (PM_{ps}) (Abugu *et al*., 2015; Chimi *et al*., 2023), but none have shown that using a chemometric tool like Response Surface Methodology (RSM) to produce activated carbons from PM_{ps} allows for its structure to be well-developed for the removal of colour in dye wastewater. Therefore, it is suggested that PM_{ps} be used as a potential precursor for H_3PO_4- and KOH-activated carbons in this study. RSM was used as a chemometric technique to optimize the production parameters (activation temperature, activation time, and impregnation ratio) to create activated carbons with well-developed porous structures. The optimized ACs (H_3PO_4-$PMAC_{op}$ and KOH-$PMAC_{op}$) were then described and used to adsorb colour from a simulated azo dye wastewater.

2 THEORETICAL ANALYSIS

Conceptual basis of the chemometric tool

The chemometric tool employed for this study is the Central Composite Rotatable Design (CCD), which is a subset of the RSM. The CCD consisted of a full two-level factorial (2^3) coded as -1 and +1 at the lower and higher levels, six (6) central replicates located at the centre (0, 0, 0) to examine experimental error and reproducibility of the data, and six (6) axial points located at (±α, 0, 0), (0, ±α, 0) and (0, 0, ±α). Alpha (α) is the distance of an axial point from the centre which makes the design rotatable and has a value of 1.68. This gives a total of 20 experimental runs.

The Central composite design

The PMACs were prepared using three independent parameters namely the activation temperature (A), activation time (B), and impregnation ratio (C). The coded and real levels of these parameters are shown in Table 1. The responses of the design were the iodine number and the carbon yield. The attributes of the experimental responses were predicted from the second-order polynomial regression model generally described by Eq. (1).

$$Y_{I_n \text{ or } C_y} = \beta_o + \sum_{i=1}^{n} \beta_i X_i + \left(\sum_{i=1}^{n} \beta_{ii} X_i\right)^2 + \sum_{i=1}^{n-1} \sum_{j=i+1}^{n} \beta_{ij} X_i X_j \qquad (1)$$

where Y is the predicted response, β_o is the constant coefficient, β_I represents the linear term coefficients, β_{ij} represents the interaction coefficients, β_{ii} represents the quadratic coefficients, X_i, X_j are the coded values of the production parameters and n is the number of variables.

The experimental sequence was randomized to minimize the effects of the uncontrolled factors and outliers. The significance of each coefficient in the models was determined by F-test and *ρ*-values. The CCD of the RSM and its corresponding statistical analyses were done using Design-Expert (10.0.0 Stat-Ease Inc., Minneapolis, MN).

Table 1: Coded and Actual Levels of Production Factors used to produce the PMACs.

Production factor	**Coded levels**				
	-α (-1.68)	-1	0	+1	+α (+1.68)
	Actual values				
Activating temperature (°C), A	200	300	450	600	700
Activating time (min), B	20	60	120	180	210
Impregnation ratio (g/L), C	1	2	3	4	5

3 EXPERIMENTAL PROCEDURE

Materials

The *Penclethra macrophylla* pods (PM_{ps}) were harvested from Benue and Enugu States – Nigeria during their peak dispersal periods from December to January. The pods were cleaned to remove dirt and sun-dried for seven (7) days to reduce their moisture contents. The biomaterials were transformed into granules using a combination of manual and mechanical size reduction mechanisms – cutting, pounding, and grinding. The PM_{ps} were passed through sieves of size 50 – 80 meshes (0.180–0.300 mm) to achieve experimental uniformity. They were stored in jute bags and labelled appropriately. Also, standard analytical grades of orthophosphoric acid 85 wt% (H_3PO_4), potassium hydroxide (KOH), Congo red ($C_{32}H_{22}N_6Na_2O_6S_2$, CR) dye, iodine, hydrochloric acid, and sodium thiosulphate were purchased and used without any further purification.

Synthesis of the activated carbons

The 85 wt% mass fractions of H_3PO_4 and 50 mg of the PM_{ps} powder were mixed according to the designed ratios of 1:1, 2:1, 3:1, 4:1, and 5:1 (volume of H_3PO_4 to the mass of PM_{ps} powder) inside some sets of steel reactors that were agitated continuously at 1000 rpm on a centrifuge for 6 hours. The PM_{ps} were filtered out of the mixtures and the samples were dried using a thermostat oven set at 110 ^oC for 1 hour to prepare the impregnated samples. The reactors were placed inside a high carbonization temperature tube furnace and heated from ambient temperature to 200 ^oC for 30 minutes, followed by further heating at the different designed temperatures ranging from 200 to 700 ^oC and activation time ranging from 20 to 210 minutes for simultaneous carbonization and activation of the precursors (Jiang *et al.*, 2019). The air within the furnace was displaced by introducing a nitrogen gas stream at 60 mL/min into it for 20 min. Similar procedures were followed to produce ACs from the PM_{ps} using KOH powder. However, the chemical impregnation of the biomaterial was done by mixing the required mass of KOH and the PM_{ps} powder to attain the designed ratios inside separate steel reactors with 30 mL of deionized water (Jiang *et al*., 2019). After the samples were dried in a thermostat oven set at 110 ^oC for 1 hour, they were transferred inside the furnace to be pyrolysed at the different designed production conditions. All the carbonized chars were allowed to cool to room temperature and thereafter washed several times with 200 mL hot and cold distilled water to achieve a neutral pH, and then allowed to dry for 2 hours at 110 ^oC using the oven. The activated carbons were boiled with HCl solution under reflux to remove impurities and reduce their inherent ash contents (Figure S1). The products pounded in a laboratory mortar and sieved using Tyler's sieves and stored in airtight containers. The dried carbon yield was determined using Eq. (2).

$$\text{Carbonyield, } C_y = (1 - m_c/m_r)100 \qquad (2)$$

where C_y is the carbon yield (%), m_c is the mass of the carbonized product (g), and m_r is the mass of precursor (g).

Characterization of the activated carbons

Determination of the iodine number

The iodine numbers of the PMACs were determined using the standard test method established by the American Society for Test and Materials (ASTM D, 2006). A 1 litre stock solution of iodine-containing 2.70 g of iodine crystals and 4.10 g of potassium iodide (KI) was prepared. It was standardized by a standard solution of sodium thiosulphate. Also, starch solution, which served as the indicator reagent was prepared by dissolving 0.30 g of starch powder in 30 mL of deionized water, and 70 mL of boiled deionized water was added to it (Pongener *et al*., 2015). For each experimental run, 0.50 g of the PMACs and 10 mL of 5%v/v HCL were introduced into a 100 mL volumetric flask. The flask was stirred gently to wet the carbon, then 100 mL of the iodine stock solution was added to the mixture and the flask was shaken on a shaker for 1 hour. The mixtures were filtered using microfibre filters, and a 20 mL aliquot portion of the filtrate was titrated with 0.10 M sodium thiosulphate, and 2 to 3 pipette drops of the starch solution was also added as an indicator (Pongener *et al*., 2015). The mixture was stirred gently until it turned colourless. The initial and final volumes of the mixture and the titre value were recorded. A blank titration procedure was similarly performed with sodium thiosulphate solution but without the addition of the PMACs. The concentration of iodine adsorbed by the PMACs at room temperature was calculated using Eq. (3).

$$I_n = [((A - B)/A) \times ((V \times M)/W)] \times 253.81 \qquad (3)$$

where I_n was the iodine number (mg/g), and A and B were the volumes of sodium thiosulphate solution required for blank and sample titrations, respectively. W is the mass of the PMACs sample, M is the molar concentration of the iodine, V is the 20 mL aliquot, and 253.81 is the atomic mass of iodine.

Morphological Assessment of the PMACs

The organic structure of the PMACs were determined using a Thermo Nicolet Fourier transform infrared spectrometer (Nicolet 67, USA). The specific area was explored through nitrogen adsorption Brunauer-Emmett-Teller BET analysis using Micrometrics 3Flex version 5.02 equipment. The textural parameters and element

constitution of the carbon were determined using scanning electron microscopy combined with energy-dispersive X-ray spectroscopy EDX.

The batch adsorption and kinetic studies of PMACs

A stock solution of the Congo Red (CR) dye was prepared as the adsorbate solution for the batch experiments. The 1000 mg/l concentration of the CR stock solution was prepared by dissolving 1.0 g of the powdered dye in 1 litre of deionized water (Hammari *et a*l., 2021). The desired concentrations of the CR dye solution for the experiments were subsequently prepared via serial dilution of the stock solution. The batch adsorption of the dyes onto the activated carbons (H_3PO_4-$PMAC_{op}$ and KOH-$PMAC_{op}$) was performed to investigate the effects of initial concentration on the adsorption profile of the carbons. The amount of the dye adsorbed by the activated carbon at each initial concentration was calculated using Eq. 4. The experimental data obtained were subsequently analysed using Origin software (version 2022) by non-linear graphical plots of the Langmuir, Freundlich, and Temkin adsorption isotherms.

$$Q_e = (100 - C_e)V/w \quad (4)$$

The effects of contact time on the adsorption profile and the kinetic parameters of the activated carbon were evaluated at 15, 30, 60, 90, 120, 150 and 180 mins using 50 mg of each activated carbon and 100 ml of 100 mg/l of the CR solution in a set of flasks placed on a rotary shaker set at 200 rpm at ambient temperature of approximately 30±2°C (Hammari *et al*., 2021). The amount of CR dyes adsorbed by the activated carbon at equilibrium at the different contact times were calculated using Eq. 5.

$$Q_t = (100 - C_t)V/w \quad (5)$$

The experimental data of the adsorption of the CR dye onto both activated carbons from the PM_{ps} was evaluated using the Pseudo-first-order (Eq. 6), Pseudo-second-order (Eq. 7), and the Elovich (Eq. 8) kinetic models to ascertain the rate-limiting profile of the adsorption process of the carbons. Nonlinear kinetics plots of the amount of CR dye adsorbed per time by both carbons were analyzed using Origin software (version 2022) as well as the experimental data and the theories of these kinetic models.

$$Q_t = Q_e(1 - e^{-K_t t}) \quad (6)$$

$$Q_t = K_2 Q_e^2 t/(1 + K_2 Q_e t) \quad (7)$$

$$Q_t = 1/\beta \ln t - 1/\beta \ln(\alpha\beta) \quad (8)$$

4 RESULTS AND DISCUSSION

Yields of the activated carbon

The optimum yields of the PMACs from the same quantity of the pods using H_3PO_4 and KOH activators differ significantly (51.10 and 39.15%, respectively). The lower AC yield of KOH-$PMAC_{op}$ is attributed to its tendency to promote intense volatilization of biomass through the breaking of C-O-C and C-C bonds (Yokoyama *et al*., 2019). Also, pyrolysis using KOH as an activator is favourable to the catalytic decomposition of heteroatoms within biomass, which promotes the increased release of gases like CO, CO_2, H_2O, and hydrocarbons, leading to lower carbon content of KOH-$PMAC_{op}$ than obtain with H_3PO_4-$PMAC_{op}$ (Jamnongkan *et al*., 2022).

Model Building and Optimization

Table 2 shows the CCD used for the experiments and the corresponding values of the responses (iodine number, I_n and carbon yield, C_y) at each experimental run for both H_3PO_4 and KOH activators. The effects of the principal factors and their interactions on each of the responses were analysed and optimized to obtain ACs with high adsorptive features. The results indicate that the three principal parameters (activation temperature, activation time, and impregnation ratio) have a high influence on the two responses for each activated carbon. The distinct variations of the I_n values, ranging from 454.74 to 1050.60 mg/g and C_y values, ranging from 29.34 to 51.30% for the KOH-PMACs and the I_n values, ranging from 217.37 to 810.06 mg/g and C_y values, ranging from 38.45 to 60.0% for H_3PO_4-PMACs are at the instant of the variations of each of these production parameters. The extent of the significant effects of these parameters on the responses is shown in Table S1. These parameters created both synergetic (positive coefficients) and antagonistic (negative coefficients) effects on the I_n and C_y values of both activated carbons, as indicated in Equations 9 to 12. However, any parameter found to be non-significant at $p>0.05$ on the ANOVA table was removed from each of the models.

$$I_{KOH} = -1108.06 + 1.52A + 6.66B + 629.66C - 2.42 \times 10^{-3}AB + 0.29AC - 1.43BC - 1.50A^2 - 88.00C^2 \quad (9)$$

$$I_{H_3PO_4} = -274.56 + 3.62A - 3.71B + 6.57 \times 10^{-3}AB - 0.17AC + 0.77BC - 3.17 \times 10^{-3}A^2 - 4.38 \times 10^{-3}B^2 - 11.35C^2 \quad (10)$$

$$C_{KOH} = 48.72 - 0.04A + 0.04B + 9.72 \times 10^{-5}AB - 3.58 \times 10^{-3}AC - 8.96 \times 10^{-3}BC - 3.38 \times 10^{-4}B^2 - 0.590C^2 \quad (11)$$

$$C_{H_3PO_4} = 46.42 - 0.02A + 0.16B - 6.17 \times 10^{-3}AC - 0.02BC - 5.02 \times 10^{-4}B^2 \quad (12)$$

With respect to the models for the iodine number of the KOH-PMACs and H_3PO_4-PMACs, the following can be inferred. Even though positive linear coefficients were clearly contributed by the three parameters to develop the KOH-PMACs of high iodine number (Equation 9), but that obtained from the impregnation ratio (+629.66) was much more profound, especially since the impregnation ratio was not significant in the preparation of the H_3PO_4-PMACs (Equation 10). Whereas the linear effects of both the activation temperature and impregnation ratio on the preparation of the KOH-PMACs and H_3PO_4-PMACs were positive coefficients, the reverse was noted for the coefficients of the interaction (AB) between these parameters. While negative coefficients of interaction between the temperature and impregnation ratio (AC) were needed to impact the iodine number of the KOH-PMACs, positive coefficients were useful to influence the iodine number of the H_3PO_4-PMACs. This implies that while a higher temperature maybe required for the simultaneous dehydration and carbonization of the KOH-impregnated PM_{ps}, a slightly lower temperature maybe needed to develop the H_3PO_4-impregnated PM_{ps}. The yields of both activated carbons were greatly influenced by both temperature and time than the impregnation ratio, as indicated by (Equations 11 and 12). Whereas both positive coefficients of interactions between temperature and time (AB) were needed to impact the yields of the KOH-PMACs and H_3PO_4-PMACs, the reverse was noticed for all the other interactions involving the impregnation ratio and the other two parameters (temperature and time), respectively.

The results (Table S2) of the numerical optimization analyses of the experimental data indicate that the PM_{ps} sample activated with H_3PO_4 at the optimum impregnation ratio of 3.7:1, temperature of 400°C, and activation time of 112 minutes recorded the highest predictive iodine number of 593.44 mg/g and carbon yield of 51.30%. The corresponding observed values recorded at these optimum conditions were 592.88 mg/g and 51.10%, respectively. For the PM_{ps} sample activated with KOH at an impregnation ratio of 3:1, temperature of 450°C, and activation time of 120 minutes, the highest predictive iodine number of 918.58 mg/g and carbon yield of 39.60% were obtained (Figure S2). An observed iodine number of 916.56 mg/g and a carbon yield of 39.15% were recorded. The specific surface areas obtained for the H_3PO_4-$PMAC_{op}$ and KOH-$PMAC_{op}$ were 527.59 and 911.70 m^2/g, respectively.

Table 2: The CCD for the Experiments and Actual and Predicted Data of the Responses obtained for both Carbons.

Run No.	A (°C)	B (min)	C (ml/g)	Iodine number, I_n (mg/g)				Carbon yield, C_y (%)			
	value & code	value & code	value & code	$PMAC_{KOH}$ observed	$PMAC_{KOH}$ predicted	$PMAC_{H3PO4}$ observed	$PMAC_{H3PO4}$ predicted	$PMAC_{KOH}$ observed	$PMAC_{KOH}$ predicted	$PMAC_{H3PO4}$ observed	$PMAC_{H3PO4}$ predicted
12	600 (+1)	180 (+1)	4 (+1)	991.96	987.62	810.06	809.83	29.43	29.52	36.37	36.34
4	600 (+1)	180 (+1)	2 (-1)	955.20	954.94	769.93	772.62	31.30	31.60	40.06	40.26
5	600 (+1)	60 (0)	4 (+1)	1026.42	1030.84	531.6	540.32	31.89	32.20	41.5	41.62
8	600 (+1)	60 (-1)	2 (-1)	653.72	656.10	683.3	687.11	32.05	32.14	40.66	40.57
6	300 (-1)	180 (+1)	4 (+1)	720.54	723.37	427.77	429.85	40.81	41.03	50.59	50.89
7	300 (-1)	180 (+1)	2 (-1)	861.11	861.91	292	289.17	40.97	40.96	51.02	51.11
2	300 (-1)	60 (-1)	4 (+1)	674.17	679.65	393.61	396.81	47.21	47.21	56.31	56.31
9	300 (-1)	60 (-1)	2 (-1)	466.57	476.13	434.01	440.13	44.78	45.00	51.33	51.57
16	700 (+1.68)	120 (0)	3 (0)	1011.64	1012.83	743.68	737.52	30.35	30.02	38.45	38.43
18	200 (-1.68)	120 (0)	3 (0)	651.34	642.64	217.37	215.06	50.44	50.33	60	59.72
20	450 (0)	210 (+1.68)	3 (0)	1050.60	1054.21	681.08	683.19	34.99	34.74	43.27	42.99
14	450 (0)	20 (-1.68)	3 (0)	794.51	784.08	591.2	581.01	39.65	39.41	46.65	46.58
19	450 (0)	120 (0)	5 (+1.68)	688.89	687.31	629.67	625.73	37.86	37.70	49.56	49.47
15	450 (0)	120 (0)	1 (-1.68)	454.74	451.11	633.79	631.84	37.72	37.57	48.76	48.64
3	450 (0)	120 (0)	3 (0)	911.43	915.95	632	644.11	39.40	39.20	46.97	47.98
10	450 (0)	120 (0)	3 (0)	950.38	915.95	658	644.11	39.33	39.20	48.41	47.98
11	450 (0)	120 (0)	3 (0)	911.43	915.95	668	644.11	39.33	39.20	48.51	47.98
1	450 (0)	120 (0)	3 (0)	911.43	915.95	642	644.11	39.98	39.20	48.86	47.98
13	450 (0)	120 (0)	3 (0)	911.43	921.21	658	674.22	39.45	40.00	48.56	49.21
17	450 (0)	120 (0)	3 (0)	911.43	921.21	668	674.22	39.30	40.00	49.01	49.21

Surface morphologies and properties of the activated carbons

The chemical activation of the PM_{ps} with H_3PO_4 and KOH showed relative variations in the textural structure of the material before and after the activation processes. The SEM micrographs of the PM_{ps} in Figure S3a revealed the large oval pores around 10 to 20 μm in diameter in the material were substantially transformed after the

chemical activation. Figure S3c for KOH-PMAC indicated its small pores while Figure S3b showed relatively larger pores in the H_3PO_4-$PMAC_{op}$. This is an indication that KOH-$PMAC_{op}$ structure contained a higher ratio of micropores than that of H_3PO_4-$PMAC_{op}$. The higher iodine numbers obtained with KOH-$PMAC_{op}$ depict availability of more microporous structure within the activated carbon and its greater affinity for the adsorption of small molecules (Karim *et al*., 2022). The extent of modification of the porous structure of the PMps and the carbons derived from them using H_3PO_4 and KOH as activating agents is shown in Figure 1a. The influence of the initial concentration of the CR dye solution on the adsorption mechanism is depicted in Figure 1b.

Adsorption study on Congo red dye

The reduction of CR dye in the solution increased with an increase in the initial concentration of the dye adsorbed onto the KOH-PMACop and H_3PO_4-$PMAC_{op}$. The obvious explanation for this phenomenon is largely that an increased concentration of the dye molecules in the solution offers them greater chance of being adsorbed onto the available adsorption sites on the carbons. This discovery is attributed to concentration gradient that drives the adsorption process (Chimi *et al*., 2023; Hammari *et al*., 2021).

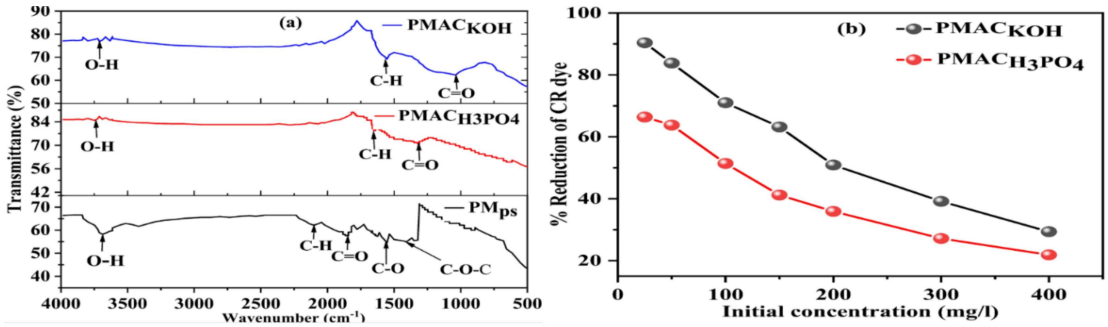

Figure 8: (a) FTIR of the PMps and the ACs by H_3PO_4 and KOH activators; (b) The effects of initial concentration on the adsorption profile of CR dye by the ACs

Also, the increased initial concentration of the CR dye solution caused the equilibrium adsorption capacities of both adsorbents to increase. This is expected, as the increased concentration of CR dye in the solution tends to overcome all resistances to mass transfer of the CR dye from the aqueous phase onto the solid phase (Hammari *et al*., 2021). The experimental data obtained for the KOH-$PMAC_{op}$ and H_3PO_4-$PMAC_{op}$ were best represented by the Langmuir isotherm (Figures 2a and b). Similarly, the Pseudo second-order kinetic model best represents the kinetic profile of the adsorption mechanism of both KOH-$PMAC_{op}$ and H_3PO_4-$PMAC_{op}$ (Figures 3a and b). The maximum amount of the CR dye adsorbed experimentally and theoretically by both activated carbons were nearly the same (Table S5).

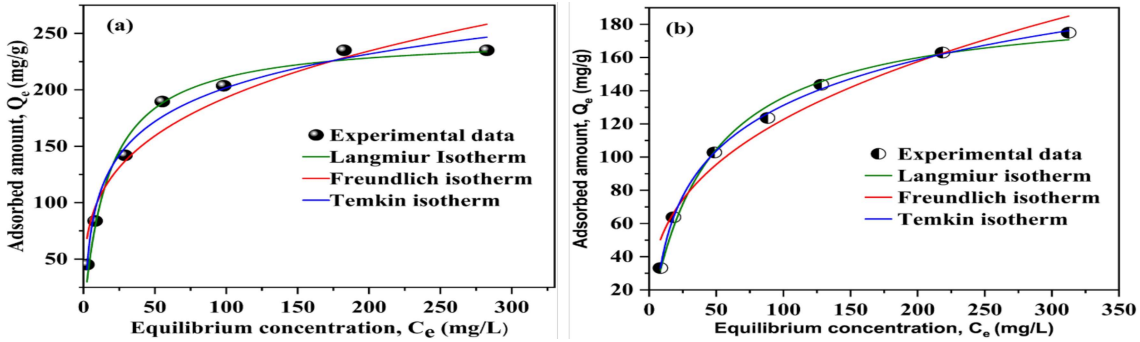

Figure 9: Adsorption isotherms of (a) KOH-$PMAC_{op}$ and (b) H_3PO_4-$PMAC_{op}$ at pH 6.8, 50 mg activated carbon, 32°C, 200 rpm and 120 minutes contact time

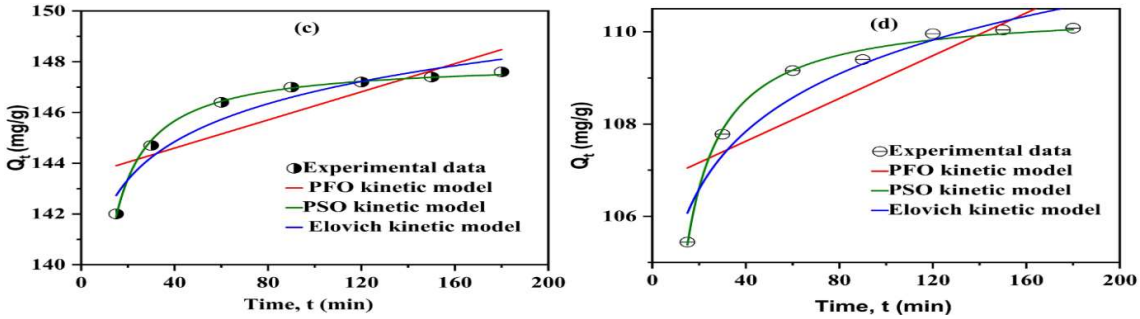

Figure 10: Adsorption kinetics of the (a) KOH-PMAC$_{op}$ and (b) H_3PO_4-PMAC$_{op}$

5 CONCLUSIONS

The RSM was used as a chemometric tool to produce activated carbons from PM$_{ps}$ with H_3PO_4 and KOH as the activating agents. The numerical optimization analyses of the experimental data indicate that the PM$_{ps}$ sample activated with H_3PO_4 at the optimum impregnation ratio of 3.7:1, temperature of 400^{o}C, and activation time of 112 minutes recorded the highest predictive iodine number of 593.44 mg/g, and carbon yield of 51.30%. The corresponding observed values recorded at these optimum conditions were 592.88 mg/g and 51.10%, respectively. For the PM$_{ps}$ sample activated with KOH at an optimum impregnation ratio of 3:1, temperature of 450^{o}C, and activation time of 120 minutes, the highest predictive iodine number of 918.58 mg/g and carbon yield of 39.60% were obtained. An observed iodine number of 916.56 mg/g and a carbon yield of 39.15% were recorded. The specific surface areas obtained for the H_3PO_4-PMAC$_{op}$ and KOH-PMAC$_{op}$ were 527.59 and 911.70 m^2/g, respectively. The Langmuir adsorption isotherm best interpreted the experimental data, and the Pseudo-second-order adsorption kinetics most suitably described the profile of the adsorption mechanism of Congo red removal by both activated carbons. The maximum amount of the CR dye adsorbed experimentally and theoretically by both activated carbons were nearly the same. Both activated carbons demonstrated evidence of extensive graphitic features from the analyses of the Raman spectroscopy and X-ray diffraction investigations conducted on them. The Fourier transform infrared (FT-IR) spectra of the KOH-PMAC$_{op}$ suggested a higher proportion of aromaticity than that of H_3PO_4-PMAC$_{op}$, which implies that it is likely to promote adsorption mechanisms like electrostatic and π-π interactions far better than that of H_3PO_4-PMAC$_{op}$.

ACKNOWLEDGEMENT

We appreciate most sincerely the technical assistance we received from the central laboratories of the Nigerian Stored Products Research Institute, Ilorin, Kwara State. We are also thankful for the support we received from the Departments of Chemistry and Animal Science, University of Agriculture, Makurdi.

REFERENCES

Abugu, H. O., Okoye, P. A. C., Ajiwe, V. I. E., Omoku, P. E., & Umeobika, U. C. (2015). Preparation and characterization of activated carbon produced from oil Bean (Ugba or Ukpaka) and snail shell. *Journal of Environmental and Analytical Chemistry*, *26*. https://doi.org/http://dx.doi.org/10.4172/jreac.1000165

Ajaelu, C. J., Oyedele, O., Ikotun, A. A., & Faboro, E. O. (2022). Safranin O dye removal using Senna fistula activated biomass: Kinetic, equilibrium and thermodynamic studies. *Journal of the Nigerian Society of Physical Sciences*, *5*, 951. https://doi.org/10.46481/jnsps.2023.951

Ao, W., Fu, J., Mao, X., Kang, Q., Ran, C., Liu, Y., & Zhang, H. (2018). Microwave assisted preparation of activated carbon from biomass : A review. *Renewable and Sustainable Energy Reviews*, *92*(July 2017), 958–979. https://doi.org/10.1016/j.rser.2018.04.051

Asaithambi, P., Yesuf, M. B., Govindarajan, R., Hariharan, N. M., Thangavelu, P., & Alemayehu, E. (2022). A Review of Hybrid Process Development Based on Electrochemical and Advanced Oxidation Processes for the Treatment of Industrial Wastewater. *International Journal of Chemical Engineering*, *2022*. https://doi.org/10.1155/2022/1105376

ASTM D, 4607-94. (2006). *Standard Test Method for Determination of Iodine Number of Activated Carbon.* West Conshohocken, PA: ASTM International.

Bilińska, L., & Gmurek, M. (2021). Novel trends in AOPs for textile wastewater treatment. Enhanced dye by-products removal by catalytic and synergistic actions. *Water Resources and Industry*, *26*(September). https://doi.org/10.1016/j.wri.2021.100160

Chandanshive, V. V., Kadam, S. K., Khandare, R. V., Kurade, M. B., Jeon, B. H., Jadhav, J. P., & Govindwar, S. P. (2018). In situ phytoremediation of dyes from textile wastewater using garden ornamental plants, effect on soil quality and plant growth. *Chemosphere*, *210*, 968–976. https://doi.org/10.1016/j.chemosphere.2018.07.064

Chimi, T., Hannah, B. U., Lincold, N. M., Jacques, M. B., Tome, S., Hermann, D. T., … Meva, F. E. (2023). Preparation, characterization and application of H3PO4-activated carbon from Pentaclethra macrophylla pods for the removal of Cr(VI) in aqueous medium. *Journal of the Iranian Chemical Society*, *20*(2), 399–413. https://doi.org/10.1007/s13738-022-02675-9

Chung, K.-T. (2016). Azo Dyes and Human Health: A Review. *Environ. Sci. Health Care*, *34*(4), 233–261. Retrieved from https://doi.org/10.1080/10590501.2016.1236602

Ekpete, O. A., Marcus, A. C., & Osi, V. (2017). Preparation and Characterization of Activated Carbon Obtained from Plantain (Musa paradisiaca) Fruit Stem . *Journal of Chemistry*, *2017*, 1–6. https://doi.org/10.1155/2017/8635615

Hammari, A. M., Misau, M. I., Aroke, U. O., Hamza, U. D., & Abdulkarim, A. (2021). Adsorption Equilibrium and Kinetics Studies of Congo Red Dye Using Groundnut Shell and Sorghum Husk Biosorbent. *Journal of Biochemistry, Microbiologiy, and Biotechnology*, *9*(1), 30–37.

Hassan, J., Rajib, M. M. R., Sarker, U., Akter, M., Khan, M. N. E. A., Khandaker, S., … Marc, R. A. (2022). Optimizing textile dyeing wastewater for tomato irrigation through physiochemical, plant nutrient uses and pollution load index of irrigated soil. *Scientific Reports*, *12*(1), 1–18. https://doi.org/10.1038/s41598-022-11558-1

Hidayu, A. R., & Muda, N. (2016). Preparation and Characterization of Impregnated Activated Carbon from Palm Kernel Shell and Coconut Shell for CO2Capture. *Procedia Engineering*, *148*, 106–113. https://doi.org/10.1016/j.proeng.2016.06.463

Jamnongkan, T., Intaramongkol, N., Kanjanaphong, N., Ponjaroen, K., Sriwiset, W., Mongkholrattanasit, R., … Huang, C. F. (2022). Study of the Enhancements of Porous Structures of Activated Carbons Produced from Durian Husk Wastes. *Sustainability (Switzerland)*, *14*(10). https://doi.org/10.3390/su14105896

Jaria, G., Silva, C. P., Oliveira, J. A. B. P., Santos, S. M., Gil, M. V., Otero, M., … Esteves, V. I. (2019). Production of highly efficient activated carbons from industrial wastes for the removal of pharmaceuticals from water—A full factorial design. *Journal of Hazardous Materials*, 212–218. https://doi.org/10.1016/j.jhazmat.2018.02.053

Jiang, W., Xing, X., Li, S., Zhang, X., & Wang, W. (2019). Synthesis, characterization and machine learning based performance prediction of straw activated carbon. *Journal of Cleaner Production*, *212*, 1210–1223. https://doi.org/10.1016/j.jclepro.2018.12.093

Kadhom, M., Albayati, N., Alalwan, H., & Al-Furaiji, M. (2020). Removal of dyes by agricultural waste. *Sustainable Chemistry and Pharmacy*, *16*(April), 100259. https://doi.org/10.1016/j.scp.2020.100259

Karim, A. Y. A., Balogoun, C., Avocefohoun, A. S., Prodjinonto, V., Gbaguidi, M. A. N., Dovonon, L. F., … Sohounhloue, D. C. K. (2022). Influence of Some Preparation Parameters on The Efficiency of Activated Carbons Prepared from Teak Wood Shavings (Tectona Grandis) and Coconut Shells (Cocos Nucifera) for The Treatment of Industrial Wastewater. *European Journal of Advanced Chemistry Research*, *3*(4), 1–9. https://doi.org/10.24018/ejchem.2022.3.4.121

Karuppasamy, K., Vikraman, D., Hussain, T., Hussain, S., Bose, R., Sivakumar, P., … Kim, H. S. (2021). Ternary Zn1-xNixSe nanostructures as efficient photocatalysts for detoxification of hazardous Congo red, methyl orange, and chrome yellow dyes in wastewater sources. *Environmental Research*, *201*(June), 111587. https://doi.org/10.1016/j.envres.2021.111587

Khan, S., & Malik, A. (2018). Toxicity evaluation of textile effluents and role of native soil bacterium in biodegradation of a textile dye. *Environmental Science and Pollution Research*, *25*(5), 4446–4458. https://doi.org/10.1007/s11356-017-0783-7

Kwiatkowski, M., & Broniek, E. (2017). An analysis of the porous structure of activated carbons obtained from hazelnut shells by various physical and chemical methods of activation. *Colloids and Surfaces A: Physicochemical and Engineering Aspects*, *529*. https://doi.org/10.1016/j.colsurfa.2017.06.028

Lam, S. S., Liew, R. K., Wong, Y. M., Yek, P. N. Y., Ma, N. L., Lee, C. L., & Chase, H. A. (2017). Microwave-assisted pyrolysis with chemical activation, an innovative method to convert orange peel into activated carbon with improved properties as dye adsorbent. *Journal of Cleaner Production*, *162*. https://doi.org/10.1016/j.jclepro.2017.06.131

Li, S., Han, K., Li, J., Li, M., & Lu, C. (2017). Preparation and characterization of super activated carbon produced from gulfweed by KOH activation. *Microporous and Mesoporous Materials*, *243*, 291–300. https://doi.org/10.1016/j.micromeso.2017.02.052

Liew, R. K., Azwar, E., Yek, P. N. Y., Lim, X. Y., Cheng, C. K., Ng, J. H., … Lam, S. S. (2018). Microwave pyrolysis with KOH/NaOH mixture activation: A new approach to produce micro-mesoporous activated carbon for textile dye adsorption. *Bioresource Technology*, *266*. https://doi.org/10.1016/j.biortech.2018.06.051

Loredo-Cancino, M. Soto-Regaldo, E. Cerino-Corfova, F.J. Garcia-Reyes, R.B., Garcia-Leon, A.M. and Garza-Gonzalez, M. T. (2013). Determining optimal conditions to produce activated carbon from barley husks using single or dual optimization. *Journal of Environmental Management*, *125*, 117–125. https://doi.org/10.1016/j.jenvman.2013.03.028

Nindjio, G. F. K., Tagne, R. F. T., Jiokeng, S. L. Z., Fotsop, C. G., Bopda, A., Doungmo, G., … Tonle, I. K. (2022). Lignocellulosic-Based Materials from Bean and Pistachio Pod Wastes for Dye-Contaminated Water Treatment: Optimization and Modeling of Indigo Carmine Sorption. *Polymers*, *14*(18). https://doi.org/10.3390/polym14183776

Ogungbenro, E.A., Quang, V.D., Al-Ali, K. and Abu-Zahra, R. M. M. (2017). Activated carbon from date seeds for CO2 capture applications. *Energy Procedia (13th International Conference on Green Gas Control Technologies GHGT-13, Lausanne, Switzerland)*, *114*, 2313–2321. https://doi.org/doi: 10.1016/j.egypro.2017.03.1370

Okpala, B. (2015). 18 reasons why you need the African oil bean (Ukpaka or Ugba). *Global Food Book*. Retrieved from https://globalfoodbook.com/health-benefits-of-african-oil-bean-seeds-ukpaka-ugba

Pongener, C., Kibami, D., Rao, K. S., Goswamee, R. L., & Sinha, D. (2015). Synthesis and Characterization of Activated Carbon from the Biowaste of the Plant Manihot Esculenta. *Chemical Science Transactions*, *4*(1), 59–68. https://doi.org/10.7598/cst2015.958

Shamsuddin, M. S., Yusoff, N. R. N., & Sulaiman, M. A. (2016). Synthesis and characterization of activated carbon produced from kenaf core fiber using H3PO4 activation. *Procedia Chemistry*, *19*, 558–565. https://doi.org/10.1016/j.proche.2016.03.053

Solayman, H. M., Hossen, M. A., Abd Aziz, A., Yahya, N. Y., Leong, K. H., Sim, L. C., … Zoh, K. D. (2023). Performance evaluation of dye wastewater treatment technologies: A review. *Journal of Environmental Chemical Engineering*, *11*(3), 109610. https://doi.org/10.1016/j.jece.2023.109610

Yang, K., Peng, J., Srinivasakannan, C., Zhang, L., Xia, H., & Duan, X. (2010). Bioresource Technology Preparation of high surface area activated carbon from coconut shells using microwave heating. *Bioresource Technology*, *101*(15), 6163–6169. https://doi.org/10.1016/j.biortech.2010.03.001

Yeow, P. K., Wong, S. W., & Hadibarata, T. (2021). Removal of azo and anthraquinone dye by plant biomass as adsorbent – a review. *Biointerface Research in Applied Chemistry*, *11*(1), 8218–8232. https://doi.org/10.33263/BRIAC111.82188232

Yokoyama, J. T. C., Cazetta, A. L., Bedin, K. C., Spessato, L., Fonseca, J. M., Carraro, P. S., … Almeida, V. C. (2019). Stevia residue as new precursor of CO2-activated carbon: Optimization of preparation condition and adsorption study of triclosan. *Ecotoxicology and Environmental Safety*, *172*(December 2018), 403–410. https://doi.org/10.1016/j.ecoenv.2019.01.096

Yorgun, S., & Yildiz, D. (2015). Preparation and characterization of activated carbons from Paulownia wood by chemical activation with H3PO4. *Journal of the Taiwan Institute of Chemical Engineers*, *53*, 122–131. https://doi.org/10.1016/j.jtice.2015.02.032

APPENDICES

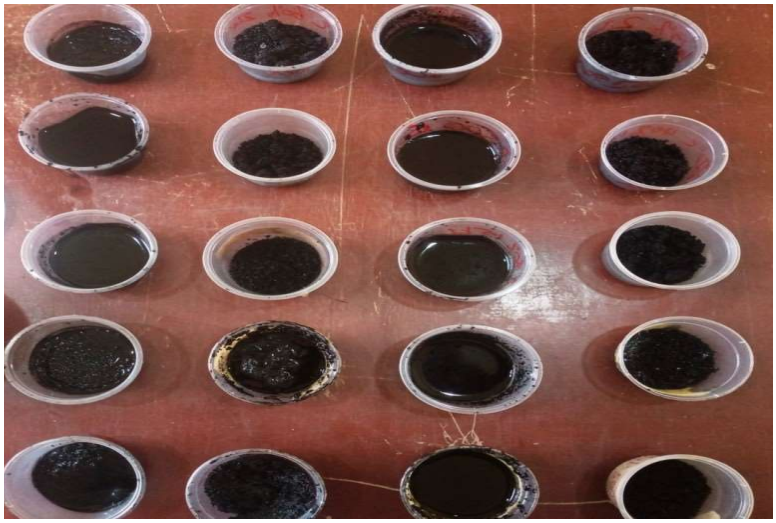

Figure S1: Acid treated and washed activated carbons

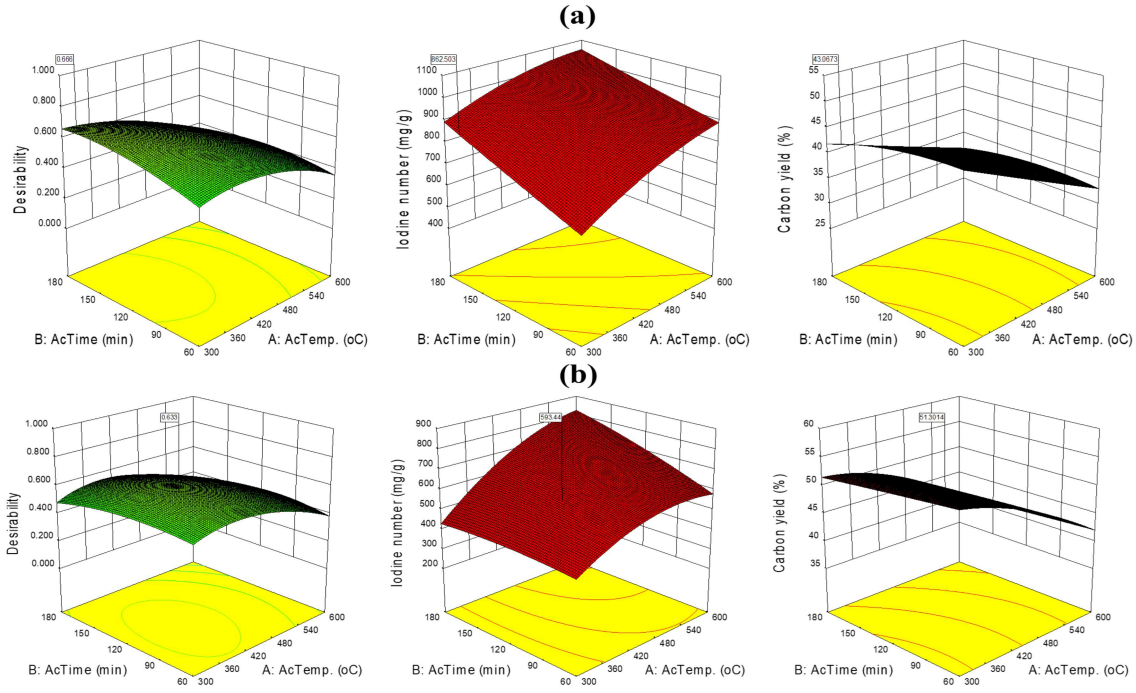

Figure S2: 3D Graphical Plots of the Effects of the pptimum production parameters on both responses (iodine number and Carbon yields) of (a) KOH-PMAC$_{op}$ and (b) H_3PO_4-PMAC$_{op}$.

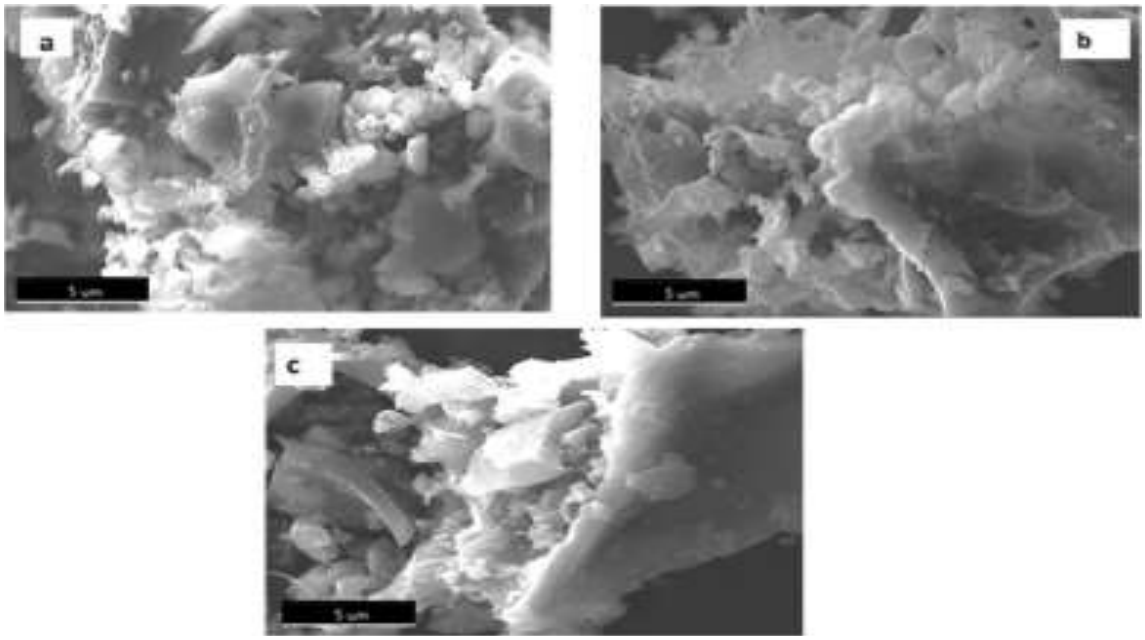

Figure S3: SE Micrographs of the (a) PMps precursor (b) H_3PO_4-$PMAC_{op}$ (c) KOH-$PMAC_{op}$

Table S3: Summary of the Results of the Analysis of Variances indicating the Significance of the Production Parameters on the Iodine number and Carbon yield of the Activated carbons

Source		Y_{In} (Iodine number)								Y_{Cy} (Carbon yield)							
	df	SS_K	SS_H	MS_K	MS_H	F_K	F_H	P_K	P_H	SS_K	SS_H	MS_K	MS_H	F_K	F_H	P_K	P_H
Model	9	598381.46	466637.83	66486.83	51848.65	327.60	302.04	0.00	4E-10	570.73	633.45	63.41	70.38	278.34	202.65	0.00	3E-09
A-act. Temp.	1	167183.06	333020.60	167183.06	333020.60	823.76	1939.97	0.00	8E-12	503.12	552.95	503.12	552.95	2208.32	1592.07	0.00	2E-11
B-act. Time	1	94734.59	11345.52	94734.59	11345.52	466.79	66.09	0.00	2E-05	36.43	26.53	36.43	26.53	159.92	76.40	0.00	1E-05
C-impreg. Ratio	1	55789.26	37.33	55789.26	37.33	274.89	0.22	0.00	7E-01	0.02	0.68	0.02	0.68	0.07	1.96	0.79	2E-01
AB	1	3779.72	27959.03	3779.72	27959.03	18.62	162.87	0.00	5E-07	6.13	0.01	6.13	0.01	26.88	0.03	0.00	9E-01
AC	1	14657.29	5353.02	14657.29	5353.02	72.22	31.18	0.00	3E-04	2.31	6.84	2.31	6.84	10.14	19.71	0.01	2E-03
BC	1	58500.81	16928.00	58500.81	16928.00	288.25	98.61	0.00	4E-06	2.31	12.35	2.31	12.35	10.14	35.56	0.01	2E-04
A2	1	15661.11	70225.26	15661.11	70225.26	77.17	409.09	0.00	8E-09	0.06	0.03	0.06	0.03	0.25	0.10	0.63	8E-01
B2	1	48.43	2958.79	48.43	2958.79	0.24	17.24	0.64	2E-03	17.64	38.92	17.64	38.92	77.42	112.07	0.00	2E-06
C2	1	197921.06	3297.18	197921.06	3297.18	975.22	19.21	0.00	2E-03	8.89	0.04	8.89	0.04	39.04	0.11	0.00	7E-01
Residual	9	1826.55	1544.96	202.95	171.66					2.05	3 Chart Area		0.35				
Lack of fit	5	688.73	718.96	137.75	143.79	0.48	0.70	0.78	7E-01	1.74	0.94	0.35	0.19	4.51	0.34	0.08	9E-01

Legend: SS_K and SS_H are the sum of square, MS_K and MS_H are the mean square, F_K and F_H are the F-calculated, and P_K and P_H are the P-values obtained from analyzing the iodine number and carbon yields of the KOH-PMAC and H_3PO_4-PMAC, respectively.

Table S4: Confirmation Tests of the Effects of the Optimum production parameters on the Activated Carbon Responses (Iodine number and Carbon yields)

Activated carbon	Parameter	Optimum	Lower	Higher	Surface area (m^2/g)
KOH-$PMAC_{op}$	Act. Temp., A	450	300	600	911.70
	Act. Time, B	120	60	180	
	Impre. ratio, C	3	2	4	
	I_n, predicted	918.58	476.13	987.6	
	I_n, observed	916.56	466.57	991.96	
	C_y, predicted	39.60	44.78	29.52	
	C_y, observed	39.15	45.00	29.43	
H_3PO_4-$PMAC_{op}$	Act. Temp., A	400	300	600	527.59
	Act. Time, B	112.45	60	180	
	Impreg. ratio, C	3.73	2	4	
	I_n, predicted	593.44	440.13	809.83	
	I_n, observed	592.88	434.01	810.00	
	C_y, predicted	51.30	51.57	36.34	
	C_y, observed	51.1	51.33	36.37	

Table S5: Effects of Initial Concentration on the Adsorption of Congo red dye from the solution

S/No.	C_o	KOH-PMAC$_{op}$		H_3PO_4-PMAC$_{op}$	
		C_e	Q_e	C_e	Q_e
1	25	2.4	45.2	8.4	33.2
2	50	8.1	83.8	18.1	63.8
3	**100**	**29**	**142**	**48.6**	**102.8**
4	150	55.2	189.6	88.2	123.6
5	200	98.2	203.6	128.2	143.6
6	300	182.5	235	218.5	163
7	400	282.5	235	312.5	175

Table S6: Effects of Contact time on the Adsorption of Congo red dye from the solution

Time (min)	C_o	KOH-PMAC$_{op}$			H3PO4-PMAC$_{op}$		
		C_t	%R	Qt	Ct	%R	2Qt
15	100	29. 00	71	142	47.28	76.36	105.44
30	100	27.65	72.35	144.7	46.11	76.945	107.78
60	100	26.80	73.2	146.4	45.42	77.29	109.16
90	100	26.50	73.5	147	45.3	77.35	109.4
120	100	26.40	73.6	147.2	45.02	77.49	109.96
150	100	26.30	73.7	147.4	44.98	77.51	110.04
180	100	26.20	73.8	147.6	44.96	77.52	110.08

Table S7: Parameters of the Theoretical Adsorption models of the isotherm and kinetics of the adsorption by both Activated Carbons

Adsorption model	Parameters	KOH-PMAC$_{op}$	H_3PO_4-PMAC$_{op}$
Langmuir	Q_m (mg/g)	248.265±8.77	194.081±5.466
	K_L (L/g)	0.057±0.009	0.0234±0.002
	R^2	0.984	0.993
	χ^2	109.906	22.407
Freundlich	K_F (L/g)	53.425±10.541	23.31±4.609
	n	3.584±0.529	2.774±0.303
	R^2	0.938	0.964
	χ^2	416.254	592.89
Temkin	A_T (L/g)	1.074±0.249	0.276±0.012
	ß	46.153±2.443	39.532±0.555
	b	54.94	64.145
	R^2	0.984	0.999
	χ^2	105.077	3.202
Pseudo-first-order (PFO) kinetic	Qe (mg/g)	143.487±0.871	106.700±0.728
	K_1 (min^{-1})	$-1.933x10^{-5}$	$-2.173x10^{-4}$
	R^2	0.7039	0.704
	χ^2	1.469	1.026
	S_{rate} ($mgg^{-1}min^{-1}$)	-0.003	-0.023
Pseudo-second-order (PSO) kinetic	Q_e (mg/g)	148.19±0.0628	110.491±0.071
	K_2 (mgg-1min-1)	0.0105	0.0124
	R^2	0.9974	0.995
	χ^2	0.0129	0.0162
	S_{rate} ($mgg^{-1}min^{-1}$)	230.583	151.38
Elovich kinetic	A_T (L/g)	$6.822x10^{-28}$	$8.051x10^{-25}$
	ß	0.4626±0.057	0.0692±0.049
	R^2	0.9309	0.9283
	χ^2	14.809	0.248